Quadripartite entangled state from cascaded second-harmonic generation*

Yang Rui(杨 瑞)[a], Zhai Shu-Qin(翟淑琴)[a)b)†], and Yang Rong-Guo(杨荣国)[a)b)]

[a)] College of Physics and Electronic Engineering, Shanxi University, Taiyuan 030006, China

[b)] State Key Laboratory of Quantum Optics and Quantum Optics Devices, Institute of Opto-Electronics, Shanxi University, Taiyuan 030006, China

(Received 16 February 2013; revised manuscript received 4 September 2013; published online 10 February 2014)

A generation system of continuous-variable (CV) quadripartite entangled state based on two cascaded second-harmonic generation (SHG) cavities below the threshold is investigated. Two reflected fundamental beams of the first cavity, the reflected second-harmonic beam and the output fourth-harmonic beam of the second cavity are proved to be entangled, and the dependence of the entanglement degree on the normalized frequency, pump parameter, fourth-harmonic loss parameter, and second-harmonic loss parameter is also analyzed. Due to the fact that the cavity parameters and the nonlinear crystals of the two SHG cavities can be freely chosen, the practicality of the proposed protocol is relatively perfect and the system can also be extended to the preparation of multicolor entangled states for a quantum network.

Keywords: harmonic generation, nonlinear optics, quantum optics, quantum communication

PACS: 42.50.–p, 42.65.–k, 42.65.Ky **DOI:** 10.1088/1674-1056/23/4/044202

1. Introduction

Entanglement, which is probably the most mysterious in all quantum phenomena, has become a key resource for the rapidly evolving quantum information technology, e.g., communication,[1] metrology,[2] and computation.[3] A variety of tasks have been performed based on multipartite entangled states, such as quantum key distribution and teleportation.[4] As a particular kind of multipartite entangled state, continuous-variable (CV) quadripartite entangled state is therefore not surprising to be able to be widely used in quantum information, especially as the quantum communication channels in numerous known teleportation protocols. Furthermore, the multipartite entangled states with different frequencies could probably be used in nodes of scalable quantum networks. On the other hand, one can experimentally establish and manipulate multipartite entanglement in microscopic systems such as photons, ions, and atoms,[5] which indeed proves that it can be generated in macroscopic and even mesoscopic systems. Moreover, multipartite entanglement reveals one of the most fascinating characteristics of quantum theory, known as the nonlocality of the quantum world.[4] Owing to its potential application in the latest development of the interdisciplinary field, it is meaningful to search a system for preparing the multipartite optical entangled states.

Until now, the schemes to generate CV multipartite entanglement have been reported in many papers. Bipartite two-color entanglement has been theoretically and experimentally realized in a regime where both parametric amplification and second harmonic generation occur.[6] The triplet photons entangled state was experimentally produced through cascaded spontaneous parametric down-conversion, the three wavelengths of the entangled state were suitable for three-party quantum communication.[7] The CV three-color entanglement produced from the type II second-harmonic generation[8,9] and cascaded NOPOs with a broad frequency choice range were theoretically investigated,[10] furthermore, the latter was realized experimentally in 2012.[11] Nowadays, CV quadripartite entanglement can generally be produced by two methods. One is to combine squeezed states of light on optical beam splitters, which leads to only entangled modes with the same frequency, for the beam splitter transformation is linear. The other is to establish entanglement with different frequencies via nonlinear optical processes.[12,13] Actually, quadripartite entanglement, as a member of multipartite entanglement, undoubtedly can store, transmit, and manipulate the quantum information with diverse frequency bands in the quantum communication networks. In addition, it is closely related to the atom system. Considering that atoms act as the ideal candidates for storage and light as the natural carrier of quantum information, light with different frequencies will be essential to connect the photonic and matter-based physical systems.[14] Hence, we consider a feasible protocol to generate a quadripartite entangled state with a broad frequency range including low-loss optical fiber transmission and atomic resonance frequencies.

Based on the above-mentioned scheme, we propose a system to generate CV quadripartite entangled optical beams, in which a pair of cascaded SHG cavities is utilized. Unlike the case using the cascaded non-linearities in just one cavity,[12,13]

*Project supported by the National Natural Science Foundation of China (Grant Nos. 61008006, 61108003, and 11274210) and the State Key Basic Research and Development Plan of China (Grant No. 2010CB923102).

†Corresponding author. E-mail: xiaozhai@sxu.edu.cn

© 2014 Chinese Physical Society and IOP Publishing Ltd

we consider two nonlinear media each in a different cavity independently, which is easily controlled in an experiment since the SHG process is relatively mature.[15] In our proposal, the second-harmonic beam output from the first type II phase-matched cavity (SHG1) is used for the pump light of the second type I phase-matched cavity (SHG2). The good phase-matching among the fundamental and harmonic fields in each SHG cavity results in the quantum correlations of the amplitude and phase quadratures between the reflect pump field and the output harmonic beams. Since the reflected second-harmonic mode and the output fourth-harmonic mode from the SHG2 both derive from the original pump beams injected into SHG1, the CV quantum correlations should exist between two reflected fundamental beams of the SHG1, the reflected second-harmonic beam and the fourth-harmonic beam of the SHG2. Generally, this type of entanglement source could aid linking together two different optical systems at diverse wavelengths and particularly bridging the gap of optical frequency between telecommunication windows and the prominent multi-level atomic systems used for quantum memories and information processing.

The rest of this paper is arranged as follows. In Section 2, a physical system of the cascaded SHG cavities for CV quadripartite entanglement generation is briefly described and the basic formulas of the field fluctuation evolution are deduced. Then the amplitude and phase quadrature fluctuations of the four modes are calculated with the boundary conditions of optical cavities. In Section 3, the criterion proposed by van Loock and Furusawa for the inseparability of optical fields is utilized to numerically analyze the entanglement characteristics of the quadripartite entangled optical state. Finally, we shall give a brief conclusion in Section 4.

2. Physical system and evolution formulas of fields

2.1. Physical model

The physical system under consideration is shown in Fig. 1. Two cascaded SHG cavities are both composed of the input and output optical couplers, between which a type II (SHG1) or a type I (SHG2) phase-matched $\chi^{(2)}$ nonlinear crystal is placed respectively. In the two SHG cavities, intracavity modes of the fundamental and the harmonic fields resonate simultaneously. Let $\hat{a}_1^{\rm in}(\omega_1)$ and $\hat{a}_2^{\rm in}(\omega_2)$ be the pump modes of SHG1, while $\hat{a}_1^{\rm out}(\omega_1)$ and $\hat{a}_2^{\rm out}(\omega_2)$ are the reflected pump modes. The output second-harmonic light $\hat{a}_0^{\rm out}(\omega_0)$ from SHG1 is used for the pump field $\hat{a}_3^{\rm in}(\omega_3)$ of SHG2, where $\hat{a}_0^{\rm out}(\omega_0)=\hat{a}_3^{\rm in}(\omega_3)$. Therefore, the pump field of SHG2 cannot be regarded as a coherent state of light as usual but as a squeezed state depending on the parameter of SHG1,[16] and the squeezing properties of the output state $\hat{a}_0^{\rm out}(\omega_0)$ from SHG1 are totally converted into SHG2 through this cascaded process. ω_i $(i=0,1,2,3,4)$ is the frequency corresponding to mode $\hat{a}_i$ $(i=0,1,2,3,4)$. Owing to the conservation of energy and momentum in the intracavity second-harmonic generation process and the mode-selecting effect of the resonant cavity, the frequencies of the intracavity modes must satisfy the relations of $\omega_0=\omega_1+\omega_2$ and $\omega_4=2\omega_3$, where $\omega_0=\omega_3$.

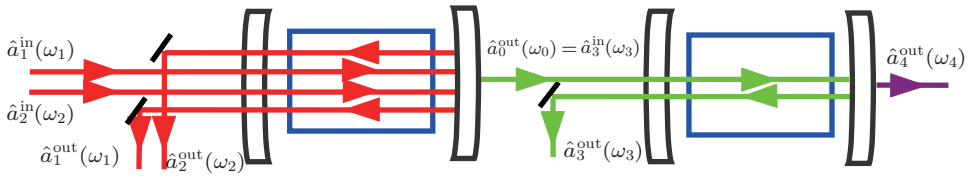


Fig. 1. (color online) A schematic illustration of the physical system for generation of a quadripartite entangled state.

2.2. Equations of motion

The system Hamiltonian for type II phase-matched SHG can be written as $\hat{H}_{\rm sys}^{II}=\hbar\omega_0\hat{a}_0^\dagger\hat{a}_0+\hbar\omega_1\hat{a}_1^\dagger\hat{a}_1+\hbar\omega_2\hat{a}_2^\dagger\hat{a}_2+{\rm i}\hbar\chi\left(\hat{a}_0\hat{a}_1^\dagger\hat{a}_2^\dagger-\hat{a}_0^\dagger\hat{a}_1\hat{a}_2\right)$, while for type I phase-matched SHG it is $\hat{H}_{\rm sys}^{I}=\hbar\omega_3\hat{a}_3^\dagger\hat{a}_3+\hbar\omega_4\hat{a}_4^\dagger\hat{a}_4+\frac{{\rm i}\hbar\kappa}{2}\left(\hat{a}_4\hat{a}_3^{\dagger 2}-\hat{a}_4^\dagger\hat{a}_3^2\right)$, where $\hat{a}_i$ $(i=0,1,2,3,4)$ is the annihilation operator of the intracavity mode corresponding to the frequency ω_i $(i=0,1,2,3,4)$, χ and κ are dimensionless nonlinear coupling coefficients of SHG processes.

Under the condition of perfect phase matching and without any detuning, the quantum Langevin equations of motion for the cascaded SHGs can be expressed as

$$\begin{aligned}
\tau\dot{\hat{a}}_0(t) &= -\gamma_0\hat{a}_0(t)-\chi\hat{a}_1(t)\hat{a}_2(t)\\
&\quad+\sqrt{2\gamma_{b0}}\hat{a}_0^{\rm in}(t)\,{\rm e}^{{\rm i}\phi_0}+\sqrt{2\gamma_{c0}}\hat{c}_0(t),\\
\tau\dot{\hat{a}}_1(t) &= -\gamma_1\hat{a}_1(t)+\chi\hat{a}_2^\dagger(t)\hat{a}_0(t)\\
&\quad+\sqrt{2\gamma_{b1}}\hat{a}_1^{\rm in}(t)\,{\rm e}^{{\rm i}\phi_1}+\sqrt{2\gamma_{c1}}\hat{c}_1(t),\\
\tau\dot{\hat{a}}_2(t) &= -\gamma_2\hat{a}_2(t)+\chi\hat{a}_1^\dagger(t)\hat{a}_0(t)\\
&\quad+\sqrt{2\gamma_{b2}}\hat{a}_2^{\rm in}(t)\,{\rm e}^{{\rm i}\phi_2}+\sqrt{2\gamma_{c2}}\hat{c}_2(t),\\
\tau\dot{\hat{a}}_3(t) &= -\gamma_3\hat{a}_3(t)+\kappa\hat{a}_4(t)\hat{a}_3^\dagger(t)\\
&\quad+\sqrt{2\gamma_{b3}}\hat{a}_3^{\rm in}(t)\,{\rm e}^{{\rm i}\phi_3}+\sqrt{2\gamma_{c3}}\hat{c}_3(t),
\end{aligned}$$

$$\tau\dot{\hat{a}}_4(t) = -\gamma_4\hat{a}_4(t) - \frac{\kappa}{2}\hat{a}_3(t)^2 + \sqrt{2\gamma_{b4}}\hat{a}_4^{\rm in}(t)\,{\rm e}^{{\rm i}\phi_4} + \sqrt{2\gamma_{c4}}\hat{c}_4(t), \quad (1)$$

where τ is the cavity round trip time and we assume it to be the same for all intracavity fields without losing generality. $\hat{a}_0(t)$, $\hat{a}_1(t)$, $\hat{a}_2(t)$, and $\hat{a}_3(t)$, $\hat{a}_4(t)$ are the annihilation operators of the intracavity fields for the SHG1 and the SHG2, respectively. $\hat{a}_0^{\rm in}(t)\,{\rm e}^{{\rm i}\phi_0}$, $\hat{a}_1^{\rm in}(t)\,{\rm e}^{{\rm i}\phi_1}$, $\hat{a}_2^{\rm in}(t)\,{\rm e}^{{\rm i}\phi_2}$, and $\hat{a}_3^{\rm in}(t)\,{\rm e}^{{\rm i}\phi_3}$, $\hat{a}_4^{\rm in}(t)\,{\rm e}^{{\rm i}\phi_4}$ are the input fields, and the initial phases of five modes are assumed to be zero. $\hat{c}_0(t)$, $\hat{c}_1(t)$, $\hat{c}_2(t)$, $\hat{c}_3(t)$, and $\hat{c}_4(t)$ are the excess vacuum noise annihilation operators. γ_{bi} $(i=0,1,2,3,4)$ and γ_{ci} $(i=0,1,2,3,4)$ represent the dimensionless damping rates associated with the amplitude transmission and reflection coefficients of the input and the output couplers of the SHG cavity and the intracavity losses, respectively. For simplicity and without losing generality, we assume that $\gamma_{b1}=\gamma_{b2}=\gamma_b$, $\gamma_{c1}=\gamma_{c2}=\gamma_c$, $\gamma_1=\gamma_2=\gamma$, where γ denotes the total damping rate of $\hat{a}_1$ and $\hat{a}_2(t)$, which satisfies $\gamma=\gamma_{bi}+\gamma_{ci}$ $(i=1,2)$. Whereas, there is $\gamma_0=\gamma_{b0}+\gamma_{c0}$ that describes the total damping rate for $\hat{a}_0(t)$.

2.3. Steady state solutions and quadrature fluctuations

Firstly, we calculate the steady-state solutions of Eq. (1) to analyze the quantum entanglement. By setting the left side of the equations to be zero, the steady-state equations with the mean-field solutions are[17]

$$\begin{aligned}
&-\gamma_0\alpha_0 - \chi\alpha_1\alpha_2 = 0,\\
&-\gamma\alpha_1 + \chi\alpha_2^*\alpha_0 + \sqrt{2\gamma_b}\beta = 0,\\
&-\gamma\alpha_2 + \chi\alpha_1^*\alpha_0 + \sqrt{2\gamma_b}\beta = 0,\\
&-\gamma_3\alpha_3 + \kappa\alpha_4\alpha_3^* + \sqrt{2\gamma_{b3}}\alpha_3^{\rm in} = 0,\\
&-\gamma_4\alpha_4 - \frac{\kappa}{2}\alpha_3^2 = 0,
\end{aligned} \quad (2)$$

where α_i $(i=0,1,2,3,4)$ and β are the mean-field solutions of the intracavity mode of $\hat{a}_i$ $(i=0,1,2,3,4)$ and the mean value of the input pump field, respectively.

Consider that the type-II SHG operates below the threshold. It is noticed that this threshold is different from the threshold of the optical parametric oscillator but a critical point where symmetry breaking occurs,[18,19] i.e., the mean value of the pump field $\alpha_3^{\rm in}$ of SHG2 is not equal to zero. Introduce the threshold $\beta^{\rm th}=\sqrt{2\gamma^3\gamma_0/\chi^2\gamma_b}$ of the type-II phase-matched SHG, and define the normalized pump parameter $\sigma=\beta/\beta^{\rm th}$, then the steady state solutions below the threshold $(\sigma<1)$ will be

$$\begin{aligned}
&\alpha_0 = -\gamma\sigma'^2/\chi,\\
&\alpha_1=\alpha_2=\sqrt{\gamma\gamma_0}\sigma'/\chi,\\
&\sigma' = \left(\sigma+\sqrt{\sigma^2+\frac{1}{27}}\right)^{1/3} - \frac{1}{3}\left(\sigma+\sqrt{\sigma^2+\frac{1}{27}}\right)^{-1/3}.
\end{aligned} \quad (3)$$

For the type-I phase-matched SHG, there is no such threshold as the type-II phase-matched SHG, under the condition of $\alpha_3^{\rm in}=\alpha_0^{\rm out}$ without a threshold, the analytical expressions of stationary solutions can be written as

$$\begin{aligned}
\alpha_3 &= \frac{(2\xi)^{1/3}}{3^{2/3}\kappa^2\chi} - \frac{2^{2/3}\gamma_3\gamma_4\chi}{(3\xi)^{1/3}},\\
\alpha_4 &= \frac{2\gamma_3}{3\kappa} - \frac{6^{1/3}\kappa\gamma_3^2\gamma_4\chi^2}{3\xi^{2/3}} - \frac{(6\xi)^{2/3}}{18\kappa^3\gamma_4\chi^2},
\end{aligned} \quad (4)$$

where

$$\xi = -9\kappa^4\gamma\gamma_4\sigma'^2\chi^2\sqrt{\gamma_0\gamma_{b3}} + \sqrt{6\kappa^6\gamma_3^3\gamma_4^3\chi^6 + 81\kappa^8\gamma^2\gamma_0\gamma_4^2\gamma_{b3}\sigma'^4\chi^4}.$$

The complete information about Gaussian states is derived from the mean values (first-order moments) and the covariance matrix (second-order moments), however, only the latter is relevant to entanglement properties. Let $\hat{a}_i(t)=\alpha_i+\delta\hat{a}_i(t)$, $\hat{a}_i^{\rm in}(t)=\alpha_i^{\rm in}+\delta\hat{a}_i^{\rm in}(t)$ $(i=0,1,2,3,4)$, and $\hat{a}_3^{\rm in}=\hat{a}_0^{\rm out}=\alpha_0^{\rm out}+\delta\hat{a}_0^{\rm out}$ where α_i is the mean value of the intracavity mode, $\delta\hat{a}_i$ $(i=0,1,2,3,4)$ is the fluctuation operator of each mode correspondingly. The pump fields of SHG1 are assumed to be coherent fields, their fluctuations are the same as the vacuum fluctuations. However, for SHG2, the pump field is the output field from SHG1, which is a squeezed field. Therefore, we can linearize the fluctuations around the steady state in Eq. (1) to obtain

$$\begin{aligned}
\tau\delta\dot{\hat{a}}_0(t) &= -\gamma_0\delta\hat{a}_0(t) - \chi\alpha_1\delta\hat{a}_2(t) - \chi\alpha_2\delta\hat{a}_1(t) + \sqrt{2\gamma_{b0}}\delta\hat{a}_0^{\rm in}(t) + \sqrt{2\gamma_{c0}}\delta\hat{c}_0(t),\\
\tau\delta\dot{\hat{a}}_1(t) &= -\gamma\delta\hat{a}_1(t) + \chi\alpha_0\delta\hat{a}_2^\dagger(t) + \chi\alpha_2\delta\hat{a}_0(t) + \sqrt{2\gamma_b}\delta\hat{a}_1^{\rm in}(t) + \sqrt{2\gamma_c}\delta\hat{c}_1(t),\\
\tau\delta\dot{\hat{a}}_2(t) &= -\gamma\delta\hat{a}_2(t) + \chi\alpha_0\delta\hat{a}_1^\dagger(t) + \chi\alpha_1\delta\hat{a}_0(t) + \sqrt{2\gamma_b}\delta\hat{a}_2^{\rm in}(t) + \sqrt{2\gamma_c}\delta\hat{c}_2(t),\\
\tau\delta\dot{\hat{a}}_3(t) &= -\gamma_3\delta\hat{a}_3(t) + \kappa\alpha_3^*\delta\hat{a}_4(t) + \kappa\alpha_4\delta\hat{a}_3^\dagger(t) + \sqrt{2\gamma_{b3}}\delta\hat{a}_0^{\rm out}(t) + \sqrt{2\gamma_{c3}}\delta\hat{c}_3(t),\\
\tau\delta\dot{\hat{a}}_4(t) &= -\gamma_4\delta\hat{a}_4(t) - \kappa\alpha_3\delta\hat{a}_3(t) + \sqrt{2\gamma_{b4}}\delta\hat{a}_4^{\rm in}(t) + \sqrt{2\gamma_{c4}}\delta\hat{c}_4(t).
\end{aligned} \quad (5)$$

For the CV, in order to obtain the entanglement characteristics of different fields, we need to investigate the fluctuations of the quadrature amplitude $\delta\hat{X}_i$ and the quadrature phase $\delta\hat{Y}_i$ $(i=1,2,3,4)$ components, where $\hat{X}$ and $\hat{Y}$ are defined by the field annihilation operator $\hat{a}$, i.e. $\hat{X}=\hat{a}+\hat{a}^\dagger$, $\hat{Y}=(\hat{a}-\hat{a}^\dagger)/{\rm i}$.

Therefore, in the frequency domain below the threshold, combining the steady state solutions (3) and (4) and Eq. (5) we have

$$M_X\begin{pmatrix}\delta\hat{X}_0(\omega)\\ \delta\hat{X}_1(\omega)\\ \delta\hat{X}_2(\omega)\\ \delta\hat{X}_3(\omega)\\ \delta\hat{X}_4(\omega)\end{pmatrix} = N_{X_1}\begin{pmatrix}\delta\hat{X}_0^{\rm in}(\omega)\\ \delta\hat{X}_1^{\rm in}(\omega)\\ \delta\hat{X}_2^{\rm in}(\omega)\\ \delta\hat{X}_3^{\rm in}(\omega)\\ \delta\hat{X}_4^{\rm in}(\omega)\end{pmatrix} + N_{X_2}\begin{pmatrix}\delta\hat{X}_{c0}(\omega)\\ \delta\hat{X}_{c1}(\omega)\\ \delta\hat{X}_{c2}(\omega)\\ \delta\hat{X}_{c3}(\omega)\\ \delta\hat{X}_{c4}(\omega)\end{pmatrix},$$

and

$$M_Y \begin{pmatrix} \delta\hat{Y}_0(\omega) \\ \delta\hat{Y}_1(\omega) \\ \delta\hat{Y}_2(\omega) \\ \delta\hat{Y}_3(\omega) \\ \delta\hat{Y}_4(\omega) \end{pmatrix} = N_{Y_1} \begin{pmatrix} \delta\hat{Y}_0^{\text{in}}(\omega) \\ \delta\hat{Y}_1^{\text{in}}(\omega) \\ \delta\hat{Y}_2^{\text{in}}(\omega) \\ \delta\hat{Y}_3^{\text{in}}(\omega) \\ \delta\hat{Y}_4^{\text{in}}(\omega) \end{pmatrix} + N_{Y_2} \begin{pmatrix} \delta\hat{Y}_{c0}(\omega) \\ \delta\hat{Y}_{c1}(\omega) \\ \delta\hat{Y}_{c2}(\omega) \\ \delta\hat{Y}_{c3}(\omega) \\ \delta\hat{Y}_{c4}(\omega) \end{pmatrix}, \tag{6}$$

with

$$M_X = \begin{pmatrix} \mathrm{i}\omega\tau+\gamma_0 & \chi\alpha_2 & \chi\alpha_1 & 0 & 0 \\ -\chi\alpha_2 & \mathrm{i}\omega\tau+\gamma & -\chi\alpha_0 & 0 & 0 \\ -\chi\alpha_1 & -\chi\alpha_0 & \mathrm{i}\omega\tau+\gamma & 0 & 0 \\ 0 & 0 & 0 & \mathrm{i}\omega\tau+\gamma_3-\kappa\alpha_4 & -\kappa\alpha_3 \\ 0 & 0 & 0 & \kappa\alpha_3 & \mathrm{i}\omega\tau+\gamma_4 \end{pmatrix},$$

$$M_Y = \begin{pmatrix} \mathrm{i}\omega\tau+\gamma_0 & \chi\alpha_2 & \chi\alpha_1 & 0 & 0 \\ -\chi\alpha_2 & \mathrm{i}\omega\tau+\gamma & \chi\alpha_0 & 0 & 0 \\ -\chi\alpha_1 & \chi\alpha_0 & \mathrm{i}\omega\tau+\gamma & 0 & 0 \\ 0 & 0 & 0 & \mathrm{i}\omega\tau+\gamma_3+\kappa\alpha_4 & -\kappa\alpha_3 \\ 0 & 0 & 0 & \kappa\alpha_3 & \mathrm{i}\omega\tau+\gamma_4 \end{pmatrix},$$

$$N_{X_1} = N_{Y_1} = \begin{pmatrix} \sqrt{2\gamma_{b0}} & 0 & 0 & 0 & 0 \\ 0 & \sqrt{2\gamma_b} & 0 & 0 & 0 \\ 0 & 0 & \sqrt{2\gamma_b} & 0 & 0 \\ 0 & 0 & 0 & \sqrt{2\gamma_{b3}} & 0 \\ 0 & 0 & 0 & 0 & \sqrt{2\gamma_{b4}} \end{pmatrix},$$

$$N_{X_2} = N_{Y_2} = \begin{pmatrix} \sqrt{2\gamma_{c0}} & 0 & 0 & 0 & 0 \\ 0 & \sqrt{2\gamma_c} & 0 & 0 & 0 \\ 0 & 0 & \sqrt{2\gamma_c} & 0 & 0 \\ 0 & 0 & 0 & \sqrt{2\gamma_{c3}} & 0 \\ 0 & 0 & 0 & 0 & \sqrt{2\gamma_{c4}} \end{pmatrix}. \tag{7}$$

Applying the boundary condition

$$\delta\hat{X}(\hat{Y})_i^{\text{out}} = \sqrt{2\gamma_{bi}}\delta\hat{X}(\hat{Y})_i - \delta\hat{X}(\hat{Y})_i^{\text{in}}$$

$(i = 1,2,3,4)$,[20] we can obtain the four output fluctuations of the quadrature amplitude and phase.

3. CV quadripartite entanglement characteristics

The quadripartite entanglement among the obtained four modes is characterized by the correlations of their quadrature amplitude and phase fluctuations. To quantify the level of correlations, we can introduce the criterion proposed by Van Loock and Furusawa[21] as follows:

$$\begin{aligned} S_1 &= \left\langle \delta^2\left(\hat{Y}_1^{\text{out}} - \hat{Y}_2^{\text{out}}\right)\right\rangle \\ &\quad + \left\langle \delta^2\left(\hat{X}_1^{\text{out}} + \hat{X}_2^{\text{out}} + g_3\hat{X}_3^{\text{out}} + g_4\hat{X}_4^{\text{out}}\right)\right\rangle \geq 4, \\ S_2 &= \left\langle \delta^2\left(\hat{Y}_1^{\text{out}} - \hat{Y}_3^{\text{out}}\right)\right\rangle \\ &\quad + \left\langle \delta^2\left(\hat{X}_1^{\text{out}} + g_2\hat{X}_2^{\text{out}} + \hat{X}_3^{\text{out}} + g_4\hat{X}_4^{\text{out}}\right)\right\rangle \geq 4, \\ S_3 &= \left\langle \delta^2\left(\hat{Y}_1^{\text{out}} - \hat{Y}_4^{\text{out}}\right)\right\rangle \\ &\quad + \left\langle \delta^2\left(\hat{X}_1^{\text{out}} + g_2\hat{X}_2^{\text{out}} + g_3\hat{X}_3^{\text{out}} + \hat{X}_4^{\text{out}}\right)\right\rangle \geq 4, \\ S_4 &= \left\langle \delta^2\left(\hat{Y}_2^{\text{out}} - \hat{Y}_3^{\text{out}}\right)\right\rangle \\ &\quad + \left\langle \delta^2\left(g_1\hat{X}_1^{\text{out}} + \hat{X}_2^{\text{out}} + \hat{X}_3^{\text{out}} + g_4\hat{X}_4^{\text{out}}\right)\right\rangle \geq 4, \\ S_5 &= \left\langle \delta^2\left(\hat{Y}_2^{\text{out}} - \hat{Y}_4^{\text{out}}\right)\right\rangle \\ &\quad + \left\langle \delta^2\left(g_1\hat{X}_1^{\text{out}} + \hat{X}_2^{\text{out}} + g_3\hat{X}_3^{\text{out}} + \hat{X}_4^{\text{out}}\right)\right\rangle \geq 4, \\ S_6 &= \left\langle \delta^2\left(\hat{Y}_3^{\text{out}} - \hat{Y}_4^{\text{out}}\right)\right\rangle \\ &\quad + \left\langle \delta^2\left(g_1\hat{X}_1^{\text{out}} + g_2\hat{X}_2^{\text{out}} + \hat{X}_3^{\text{out}} + \hat{X}_4^{\text{out}}\right)\right\rangle \geq 4, \end{aligned} \tag{8}$$

where S_i $(i = 1,2,3,4,5,6)$ represents the quantum correlation spectrum of the output field, $\hat{X}_j^{\text{out}}$ and $\hat{Y}_j^{\text{out}}$ $(j = 1,2,3,4)$ are the quadrature amplitude and phase operators of the output fields, and g_k $(k = 1,2,3,4)$ is the scaling factor to minimize the combined correlation variance S_i.

To demonstrate the full inseparability of the quadripartite system, we must rule out any of the partially separable forms, which requires violating at least three inequalities of the above six inequalities in Eq. (8).[12] These three are available to reach the aim

$$\begin{aligned} S_1 &= \left\langle \delta^2\left(\hat{Y}_1^{\text{out}} - \hat{Y}_2^{\text{out}}\right)\right\rangle \\ &\quad + \left\langle \delta^2\left(\hat{X}_1^{\text{out}} + \hat{X}_2^{\text{out}} + g_3\hat{X}_3^{\text{out}} + g_4\hat{X}_4^{\text{out}}\right)\right\rangle \geq 4, \\ S_2 &= \left\langle \delta^2\left(\hat{Y}_1^{\text{out}} - \hat{Y}_3^{\text{out}}\right)\right\rangle \\ &\quad + \left\langle \delta^2\left(\hat{X}_1^{\text{out}} + g_2\hat{X}_2^{\text{out}} + \hat{X}_3^{\text{out}} + g_4\hat{X}_4^{\text{out}}\right)\right\rangle \geq 4, \\ S_6 &= \left\langle \delta^2\left(\hat{Y}_3^{\text{out}} - \hat{Y}_4^{\text{out}}\right)\right\rangle \end{aligned}$$

$$+\left\langle \delta^2\left(g_1\hat{X}_1^{\text{out}}+g_2\hat{X}_2^{\text{out}}+\hat{X}_3^{\text{out}}+\hat{X}_4^{\text{out}}\right)\right\rangle \geq 4,$$

Employ the experimentally reachable system parameters in the numerical calculation. The quantum correlation spectra of the four modes described by S_1, S_2, and S_6 versus normalized frequency $\Omega = \omega\tau/\gamma$ are plotted in Fig. 2. The results show that all the values of S_1 (solid curve), S_2 (dashed curve), and S_6 (dash–dotted curve) are below a quantum limit of 4 in a wide frequency range, which satisfies the above inseparability criterion for CV quadripartite entanglement. In addition, because of the cascaded process, the maximum correlation is obtained at about $\Omega = 1.5$. It is obviously seen that S_1 generated from SHG1 is smaller than the other two pairs.

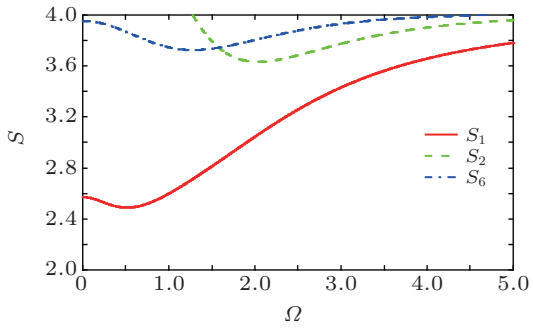


Fig. 2. (color online) Quantum correlation spectra S_1 (solid curve), S_2 (dashed curve), S_6 (dash–dotted line) versus normalized frequency $\Omega = \omega\tau/\gamma$, with $\gamma = 0.038$, $\gamma_b = 0.0342$, $\gamma_0 = 0.09$, $\gamma_{b0} = 0.081$, $\gamma_3 = 0.038$, $\gamma_{b3} = 0.0342$, $\gamma_4 = 0.09$, $\gamma_{b4} = 0.081$, $\chi = \kappa = 1$, and $\sigma' = 0.65$.

The quantum correlation spectra of S_1 (solid curve), S_2 (dashed curve), and S_6 (dash–dotted curve) versus pump parameter σ' related to the threshold and the pump power density are plotted in Fig. 3. It shows that the best correlations for all the four modes can be obtained around $\sigma' = 0.65$. The CV quadripartite entanglement generated from the nonlinear cascaded SHGs operating below the threshold can be realized within a wide power range by choosing appropriate system parameters. The correlation spectrum S_1 is smaller than the other two correlation spectra S_2 and S_6. Moreover, S_1 is up to the best value near the region of the threshold point.

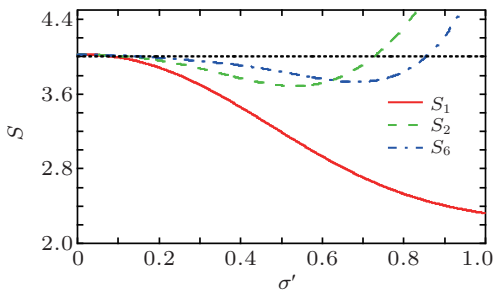


Fig. 3. (color online) Quantum correlation spectra S_1 (solid curve), S_2 (dashed curve), S_6 (dash–dotted line) versus pump parameter σ', with $\gamma = 0.038$, $\gamma_b = 0.0342$, $\gamma_0 = 0.09$, $\gamma_{b0} = 0.081$, $\gamma_3 = 0.038$, $\gamma_{b3} = 0.0342$, $\gamma_4 = 0.09$, $\gamma_{b4} = 0.081$, $\chi = \kappa = 1$, and $\Omega = 1.5$.

For searching the optimal operation conditions and the cavity parameters of the cascaded SHG system, the cavity parameters should be taken into account. We show the dependences of the three correlation spectra S_1 (solid curve), S_2 (dashed curve), and S_6 (dash–dotted curve) versus the fourth-harmonic loss parameter γ_4 of the SHG2 in Fig. 4. As shown in this figure, S_1, S_2, and S_6 violate the inequalities over quite a large region. The realization of quadripartite entanglement displayed in the figure also shows the transfer of energy from SHG1 to SHG2 by the cascaded process.

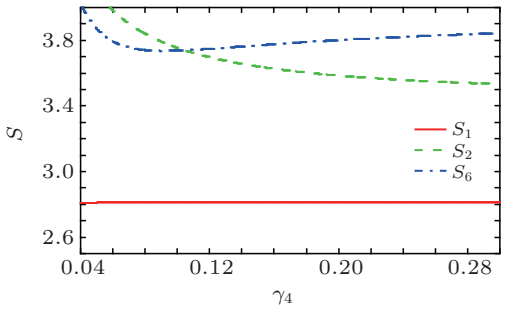


Fig. 4. (color online) Quantum correlation spectra S_1 (solid curve), S_2 (dashed curve), S_6 (dash–dotted line) versus fourth-harmonic loss parameter γ_4 for the system below threshold, with $\gamma = 0.038$, $\gamma_b = 0.0342$, $\gamma_0 = 0.09$, $\gamma_{b0} = 0.081$, $\gamma_3 = 0.038$, $\gamma_{b3} = 0.0342$, $\sigma' = 0.65$, $\chi = \kappa = 1$, and $\Omega = 1.5$.

Since the output second-harmonic state $\hat{a}_0^{\text{out}}$ of SHG1 is used for the pump mode $\hat{a}_3^{\text{in}}$ of SHG2, the degree of quadripartite entanglement is closely associated with the middle state $\hat{a}_0^{\text{out}}$ $(\hat{a}_3^{\text{in}})$, which is deeply influenced by the second-harmonic loss parameter γ_0. The system parameter γ_0 describing the total damping rate of the second-harmonic light $\hat{a}_0$ should be comprehensively considered to achieve the optimal entanglement. We numerically calculate the three correlation spectra S_1 (solid curve), S_2 (dashed curve), and S_6 (dash–dotted curve) versus system parameter γ_0 and plot them in Fig. 5. The figure shows that by choosing the appropriate value of γ_0, the criterion for the quadripartite entanglement is satisfied, i.e., S_1, S_2, and S_6 are below 4.

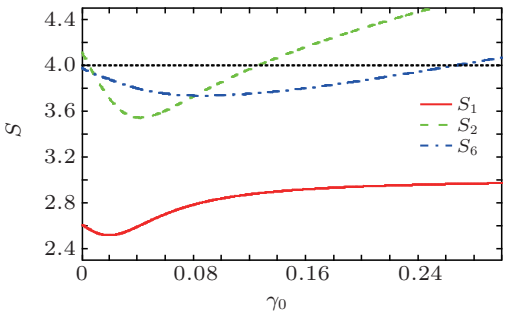


Fig. 5. (color online) Quantum correlation spectra S_1 (solid curve), S_2 (dashed curve), S_6 (dash–dotted line) versus second-harmonic loss parameter γ_0 for the system below threshold, with $\gamma = 0.038$, $\gamma_b = 0.0342$, $\gamma_3 = 0.038$, $\gamma_{b3} = 0.0342$, $\gamma_4 = 0.09$, $\gamma_{b4} = 0.081$, $\sigma' = 0.65$, $\chi = \kappa = 1$, and $\Omega = 1.5$.

4. Conclusion

In this paper, we proposed a scheme to generate a CV quadripartite entangled state in which two cascaded SHG cavities are used. According to the results, we show that the expected CV genuine quadripartite entanglement exists in the cascaded SHG system under some reachable conditions, which provides a direct reference for the design of experimental systems. This type of entanglement source bridges the octave in optical frequency between the atomic transition ($\sim$ 0.4 μm) and telecommunication windows (0.8 μm $\sim$ 1.6 μm) used in quantum information processing. Moreover, our protocol can be easily extended to the striking investigation into the entanglement of an atom and its spontaneous emission,[22] as well as the entanglement evolution between atoms and the quantized field in the Jaynes–Cummings model.[23,24] Because of the nonlinear crystals and the cavity parameters of two SHG cavities, which can be flexibility chosen, we combine the multiple conversion idea in a subharmonic-pumped parametric oscillator operating above the threshold presented in Ref. [25] to generate a CV quadripartite entangled state of a very broad wavelength range. Meanwhile, a compact way to generate multicolor CV quadripartite entanglement with a wide frequency range is presented, which is actually significant for the applications in quantum information networks.

References

[1] Kalev A, Mann A and Revzen M 2013 *Phys. Rev. Lett.* **110** 260502
[2] Kimble H J 2008 *Nature* **453** 1023
[3] Zhang D Y and Zhan M S 1999 *Chin. Phys.* **8** 269
[4] Ramzan M 2012 *Chin. Phys. Lett.* **29** 020302
[5] Ma Y H and Zhou L 2013 *Chin. Phys. B* **22** 024204
[6] Grosse N B, Bowen W P, McKenzie K and Lam P K 2006 *Phys. Rev. Lett.* **96** 063601
[7] Hübel H, Hamel D R, Fedrizzi A, Ramelow S, Resch K J and Jennewein T 2010 *Nature* **466** 601
[8] Zhai S Q, Yang R G, Liu K, Zhang H L, Zhang J X and Gao J R 2009 *Opt. Express* **17** 9851
[9] Zhai S Q, Yang R G, Fan D H, Guo J, Liu K, Zhang J X and Gao J R 2008 *Phys. Rev. A* **78** 014302
[10] Tan A H, Xie C D and Peng K C 2012 *Phys. Rev. A* **85** 013819
[11] Jia X J, Yan Z H, Duan Z Y, Su X L, Wang H, Xie C D and Peng K C 2012 *Phys. Rev. Lett.* **109** 253604
[12] Leng H Y, Wang J F, Yu Y B, Yu X Q, Xu P, Xie Z D, Zhao J S and Zhu S N 2009 *Phys. Rev. A* **79** 032337
[13] Guo J, Zhai Z H and Gao J R 2010 *J. Opt. Soc. Am. B* **27** 518
[14] Coelho A S, Barbosa F A S, Cassemiro K N, Villar A S, Martinelli M and Nussenzveig P 2009 *Science* **326** 823
[15] Andreev Y, Geiko P, Lanskii G, Badikov V, Ren D M, Hu X Y, Qu Y C and Huang J Z 2004 *Acta Phys. Sin.* **53** 3761 (in Chinese)
[16] Zhai S Q and Guo J 2011 *Acta Sin. Quantum Opt.* **17** 3 (in Chinese)
[17] Reynaud S, Fabre C and Giacobino E 1987 *J. Opt. Soc. Am. B* **4** 1520
[18] Jack M W, Collett M J and Walls D F 1996 *Phys. Rev. A* **53** 1801
[19] Longchambon L, Treps N, Coudreau T, Laurat J and Fabre C 2005 *Opt. Lett.* **30** 284
[20] Collett M J and Gardiner C W 1984 *Phys. Rev. A* **30** 1386
[21] van Loock P and Furusawa A 2003 *Phys. Rev. A* **67** 052315
[22] Tan L, Zhang Y Q and Zhu Z H 2011 *Chin. Phys. B* **20** 070303
[23] Ouyang X C, Fang M F, Kang G D, Deng X J and Huang L Y 2010 *Chin. Phys. B* **19** 030309
[24] Li G X and Peng J S 1997 *Chin. Phys.* **6** 97
[25] Schneider K and Schiller S 1997 *Opt. Lett.* **22** 363